Pharmaceutical Research, Vol. 26, No. 5, May 2009 (© 2009)
DOI: 10.1007/s11095-009-9837-y

Research Paper

Design of a Multifunctional PLGA Nanoparticulate Drug Delivery System: Evaluation of its Physicochemical Properties and Anticancer Activity to Malignant Cancer Cells

Zhe Wang,[1] Wai-Keung Chui,[1] and Paul C. Ho[1,2]

Received November 19, 2008; accepted January 14, 2009; published online February 4, 2009

Purpose. Several individual approaches were combined to fabricate a novel nanoparticulate drug delivery system to achieve targeting and anticancer effects in various malignant cancer cells.
Methods. Doxorubicin was conjugated to Poly(lactic-*co*-glycolic acid) (PLGA), which was formulated into nanoparticle via solvent-diffusion method. The surface of the nanoparticles was subsequently linked with Poly(ethylene glycol) (PEG) and Arg-Gly-Asp (RGD) peptide to realize both passive and active targeting functions. The multifunctional nanoparticles were then tested against several malignant cancer cell lines.
Results. The conjugation increased loading efficiency of doxorubicin to PLGA nanoparticles (the encapsulation efficiency was over 85%) and alleviated the drug burst release effect substantially. The drug was released from the polymeric matrix in a sustained release manner over a period of 12 days. The resultant nanoparticles were spherically uniform and well-dispersed. The nanoparticle targeting ability was proven through strong affinity to various *integrin*-expressing cancer cells, and much less affinity to the low *integrin* expression cancer cells. The nanoparticles also showed high efficacy in inducing apoptosis in specific malignant cancer cell.
Conclusion. The developed multifunctional nanoparticles hold potential to treat malignant *integrin*-expressing cancers.

KEY WORDS: cancer; drug delivery; integrin; multifunctional; nanoparticle.

INTRODUCTION

Most cancers begin as localized diseases, but they are prone to spread to distant sites within the body. This adverse character makes many cancers incurable. The adhesion molecules were reported to play key roles in the regulation of cellular activation, migration, proliferation, survival, apoptosis, and differentiation (1,2). The overexpression of *integrin* receptors on some malignant cancer cells provides a distinct marker for targeted chemotherapeutical or diagnostic contrast agent deliveries. Typically, the Arg-Gly-Asp (RGD) peptide, which has high affinity to αvβ3 *integrin*, has been applied in experimental studies to deliver either drugs (3), gene (4) or imaging agents (5) to the desired targeted sites (6,7).

Nanoparticulate drug delivery system has been extensively explored in the past few decades, and the technology is rapidly advancing (8). Thus, the emerging nanomedicine in cancer therapy is popularly explored by many researchers (9–11). Since most of the current chemotherapeutical drugs have notoriously undesirable side effects, which limit their further clinical application, novel drug delivery system aiming to overcome the intrinsic side effects arising from the anticancer drugs are urgently needed. Site specific targeting nanoparticles are evidenced to be a promising tool to effectively deliver anticancer drugs (12–14). Some targeting peptides, like RGD, are also considered as promising ligands for targeted delivery payloads to specific malignant cancer cells. Nevertheless, active targeting function is hardly successfully accomplished until the passive targeting function is realized (15). Poly(ethylene glycol) (PEG) for passive targeting goal is much favored by many researchers due to its biocompatibility, degradability, and less protein interaction characters in animal body (16). Thus, nanoparticles assembling both passive and active targeting functions hold great potential in clinical application.

Poly(lactic-*co*-glycolic acid) (PLGA) was regarded as biological friendly and degradable materials in biomedical application. And many investigations have been done to use PLGA as matrix material to deliver drug, gene or imaging agents. Nevertheless, most of the PLGA micro- or nanoparticles were short of either passive or active targeting function, or both of them. Also, the inevitable burst release effect involved in PLGA based nanoparticulate delivery systems sets another hurdle for its clinical application.

Here, we reported PLGA based nanoparticles with surface modification of PEG and targeting peptide cRGD for simultaneous passive and active targeting functions.

[1] Department of Pharmacy, National University of Singapore, 18 Science Drive 4, Singapore, 117543, Singapore.
[2] To whom correspondence should be addressed. (e-mail: phahocl@nus.edu.sg)

PLGA was chemically conjugated with doxorubicin, a widely used anticancer drug, before it was fabricated into nanoparticles to avoid the burst effect commonly observed in nanoparticles physically loaded with therapeutic drugs (17,18). The physicochemical properties of the nanoparticles were characterized. The selective uptake of these Doxo-PLGA-PEG-cRGD nanoparticles by different cancer cells was investigated via flow cytometry and confocal laser scanning microscope (CLSM). The potency to induce apoptosis in malignant cancer cell was initially evaluated by DNA fragmentation assay and western blot assay.

MATERIALS AND METHODS

Materials

PLGA (RG503H) was obtained from Boehringer Ingelheim (Germany). Amino-Poly (ethylene glycol)-Carboxylic acid (NH_2-PEG-COOH) with M.W. 2000 was purchased from NOF Corporation, Japan. Poly (ethylene-maleic anhydride) (PEMA) was purchased from Polysciences, Inc. *N*-hydroxysuccinimide (NHS), *N*-(3-Dimethylaminopropyl)-*N′*-ethylcarbodiimide hydrochloride (EDC), 4-Nitrophenyl chloroformate (pNC), pyridine, acetone, triethylamine (TEA), *N*,*N*-Dimethylformamide (DMF), 3-(4,5-dimethylthiaol-2-yl)-2,5-diphenyltetrazolium bromide (MTT), Dulbecco's Modified Eagle's Medium (DMEM) and RPMI-1640 medium were purchased from Sigma Chemical, Co (St. Louis, MO, USA). All other chemicals were of analytical grade. Doxorubicin hydrochloride was purchased from Woo-Shin Medics, Co. Korea. B16F10 mouse melanoma cells, DU145 human prostate carcinoma cells, MDA-MB-231 human mammary carcinoma cells, and MCF-7 human mammary carcinoma cells were obtained from American Type Culture Collection (Rockville, MD). Antibodies used in western blot were purchased from Cell Signaling Inc. All other chemicals used in this study were obtained from Sigma, Co. (MO, USA). Deionized water (Millipore, Bedford, MA, USA) was used thorough the entire study.

Conjugation of Doxorubicin to PLGA

PLGA (Resome® 503H), with a lactide/glycolide molar ratio of 50/50, and free hydroxyl and carboxylic groups at its terminal ends, was used. The preparation procedure was similar to a previous study (19) with minor modification. Briefly, 0.5 g of PLGA was dissolved in 10 ml of methylene chloride and activated by the addition of 26.3 mg of p-nitrophenyl chloroformate and 18 μL of pyridine to the solution, kept in an ice bath at 0°C. After isolation, 0.3 g activated PLGA was dissolved in 3 mL of dimethylformamide (DMF) and reacted with 12.9 mg of doxorubicin with 15.5 μL of triethylamine for 24 h at room temperature under nitrogen atmosphere. The final conjugated product was precipitated by excess cold ether, and dried under vacuum. The efficiency of doxorubicin conjugated to PLGA was determined by dissolving the conjugated products in DMSO, and the amount of doxorubicin was quantitated by UV/VIS spectrometry (Perkin-Elmer, Japan) at 480 nm.

Preparation of PLGA-doxorubicin (PLGA-Doxo) Nanoparticles

PLGA nanoparticles were prepared by a solvent diffusion method (20). 50 mg of PLGA-doxorubicin conjugate was dissolved in 3.5 mL of acetone, and the organic solution was added to 0.2% PEMA (35 mL) through a syringe pump (20 mL/h) under stirring at 1,500 rpm in a fume hood to evaporate acetone overnight. The nanoparticles produced were collected and washed three times with deionized water, and followed by ultrafiltration (Millipore, Amicon®) at 4,000 rpm for 45 min. Finally, the nanoparticles were dispersed in deionized water to give the desired concentration.

Synthesis of Doxo-PLGA-PEG-cRGD Nanoparticles

Ten milliliters of the prepared PLGA-Doxo nanoparticle solution was diluted with 0.1 M MES (pH 6.0), and then subject to ultrafiltration, and washed with 0.1 M MES twice. The precipitated nanoparticles were collected, and finally suspended in 0.1 M MES solution. 153 mg EDC, and 230 mg sulfo-NHS were added into the nanoparticle suspension. The mixture was incubated for 2 h at room temperature. After washing off the impurities from the suspension with PBS buffer (pH 7.4), 50 mg NH_2-PEG-COOH with 6.9 μl TEA was introduced into the activated PLGA-Doxo nanoparticle suspension, and incubated for 4 h. The resultant product was washed three times with PBS (pH 7.4) and separated by ultrafiltration. Finally, the nanoparticles were dispersed in PBS buffer to the desired concentration.

The prepared PLGA-PEG nanoparticles were once again diluted, washed, and suspended in 0.1 M MES (pH 6.0) for another cycle EDC/NHS chemistry for conjugation of cRGD peptide. The activated PLGA-PEG nanoparticle suspension was mixed with 1.5 mg cRGD (Anaspec, USA), and incubated overnight for complete reaction. After that, the synthesized Doxo-PLGA-PEG-cRGD nanoparticles were dispersed in PBS (pH 7.4) buffer to the desired concentration.

Characterization of Nanoparticles

The mean size, polydispersity and zeta potential of the NPs were determined by size analyzer (Zetasizer 3000 HSA, Malvern Instruments Ltd., England).The encapsulated drug in the NPs and drug encapsulation efficiency were determined via spectrometry under 480 nm with microplate reader. The spectrometry was calibrated with different concentrations of doxorubicin dissolved in DMSO. The cRGD peptide conjugated on the nanoparticle surface was calculated with the established fluorescamine method (21). The micro-structure of the NPs was visualized by transmission electron microscopy (TEM) (CM10, Microscope Philips) with 2% phosphotungstic acid staining.

Cytotoxicity Assay

The cell proliferation assay was conducted based on tetrazolium dye (MTT) method. MDA-MB-231, B16F10 and MCF-7 cells were grown in DMEM medium, and DU-145 cells were grown in RPMI-1640 medium. All the cell culture

media were supplemented with 10% FBS, 0.1% nonessential amino acids, and 100 μg/ml penicillin, and 100 unit/ml streptomycin. The cells were separately seeded into 96-well plates at the density of 5×10^3 cells/well and incubated at 37 °C, 5% CO_2 for 24 h before experiment. NPs were diluted with corresponding culture media to different concentrations. Pure drug was used as control. After washing the cells with PBS buffer three times, different concentrations of samples were added to the respective cells at 200 μL/well. After incubation for 48 h, the cells were washed with PBS buffer three times, and further incubated with 120 μL/well MTT solution (0.5 mg/ml) for another 3 h. At the end of incubation time, the excess MTT solution was removed, and the formed formazan crystals were dissolved by DMSO. The resultant solution was measured at 570 nm with DMSO as blank (n=6).

Cell Uptake and Binding Affinity Assays

Since doxorubicin is intrinsically fluorescent, this facilitated the visualization of the uptake of the doxorubicin formulated NPs into cells under confocal laser scanning microscope (CLSM). To observe the internalization of NPs under CLSM, the desired cells were cultured over night in Lab-Tek® eight well chambers (Nalgene, Nunc Inc., Denmark; seeded at density of 2.0×10^4 cells/well). Then, the cells were washed with 3×0.2 mL/well of PBS and equilibrated with 0.2 mL/well of HBSS/HEPES at 37°C for 30 min. Freshly prepared nanoparticles were diluted with HBSS/HEPES to give the desired concentrations. After balancing the cells with HBSS/HEPES, the medium was then aspirated, and 200 μL/well NPs solution was added into each well. At different time points, the uptake experiment was terminated by aspirating the test samples and washing the cell monolayers with 0.2 mL/well of ice-cold PBS three times. Then, each cell monolayer was fixed with methanol/acetone (1:1, v/v) followed by nuclear staining with DAPI (20 μmol/mL). The cells were observed under CLSM (Zeiss, Heidelberg, Germany) with excitation filter at 488 nm, long band pass emission filter 520 nm for internalized drug; and UV excitation for DAPI staining.

DNA Fragmentation Assay

DNA fragmentation assay was performed on MDA-MB-231 cells, according to the procedure previously described procedure (22) with minor modification. Cells were grown in DMEM medium before treatment. On the experimental day, cells were treated with 1) cell culture medium; 2) pure drug dissolve in cell culture medium (5μg/ml), and 3) Doxo-PLGA-PEG-cRGD nanoparticle with equivalent drug concentration in culture medium. After 48 h incubation, cells were washed with ice-cold PBS three times and collected by trypsinization. The cell pellets were re-suspended in 0.5 ml lysis buffer (1% Triton X-100 with 20 mM EDTA and 50 mM Tris–HCl, pH 7.4). The supernatant was subjected to 5 mg/ml RNase A at 56°C for 2 h, followed by incubation with 2.5mg/ml Proteinase K for at least 2 h at 37°C. After addition of 0.5 volume of 10 M ammonium acetate, DNA was precipitated with 2.5 volume of absolute ethanol at −20°C overnight. Then, the DNA was collected via high speed centrifugation, and rinsed with 70% ethanol once, and the DNA pellets were collected after centrifugation for 25 min at 14,000 rpm. The retrieved pellet was dried in a SpeedVac to remove the residual ethanol. The resultant DNA was dissolved in TE buffer (10mM Tris–HCl and 1mM EDTA, pH 8.0), followed by 1% agarose gel electrophoresis, and stained with ethidium bromide.

Western Blot Analysis

Western blot analysis was conducted on MDA-MB-231 cells. Protein was extracted from cells with lysis buffer (1% Triton X-100 with Proteinase inhibitor cocktail) at 4°C. The extracted proteins were separated with SDS-PAGE and transferred to PVDF membrane. The membrane was blocked by TBS buffer containing 5% skim milk over night. After washing with washing buffer (TBS buffer with 0.1% Tween 20), the membrane was incubated with primary antibodies specific for cleaved, non-cleaved caspases 3 and actin at room temperature for 2 h, and corresponding secondary antibodies for 1 h. After extensive washing, bands were detected by FluroChem® imaging system (Alpha Innotech, CA, USA).

Determination of Doxo-PLGA-PEG-cRGD Nanoparticle Uptake by Flow Cytometry

MDA-MB-231 cells were grown in confluent condition. Doxo-PLGA-PEG-cRGD nanoparticles were diluted to the desired concentrations with HBSS buffer, and incubated with cells for 4 h. The cells were then washed three times with ice-cold PBS and trypsinized. The cell pellets were further washed with ice-cold PBS twice, and 1 ml 70% ethanol was added to fix the cells at −20°C overnight. The cells were washed once again before flow cytometry (Dako, USA) analysis.

In vitro Drug Release

In vitro drug release profile of Doxo-PLGA-PEG-cRGD nanoparticles was determined by loading 1 ml of original nanoparticle solution into dialysis tubing (M.W. 12,000), which was submerged into 10 ml PBS (pH 7.4), and shaken at 37°C, 100 rpm in a water bath. The released drug was retrieved at pre-determined time points, and analyzed by fluorescence spectrometry (λ_{ex}=480 nm; λ_{em}=590 nm).

RESULTS

Conjugation of Doxorubicin to PLGA

The conjugation of doxorubicin to biodegradable, biocompatible polymer, PLGA, has been reported to be effective in enhancing the drug bioavailability, minimizing the burst release effect and substantially enhancing the loading efficiency (17–19). Fig. 1 shows the schematic route of doxorubicin-PLGA conjugation by carbamate linkage between the hydroxyl group on PLGA and amine group on doxorubicin. The available carboxyl groups were ready for the subsequent linkage with the primary amine groups on PEG chain after formation of nanoparticles. The extent of conjugation of doxorubicin to the PLGA was determined to be around 2.93% in weight ratio.

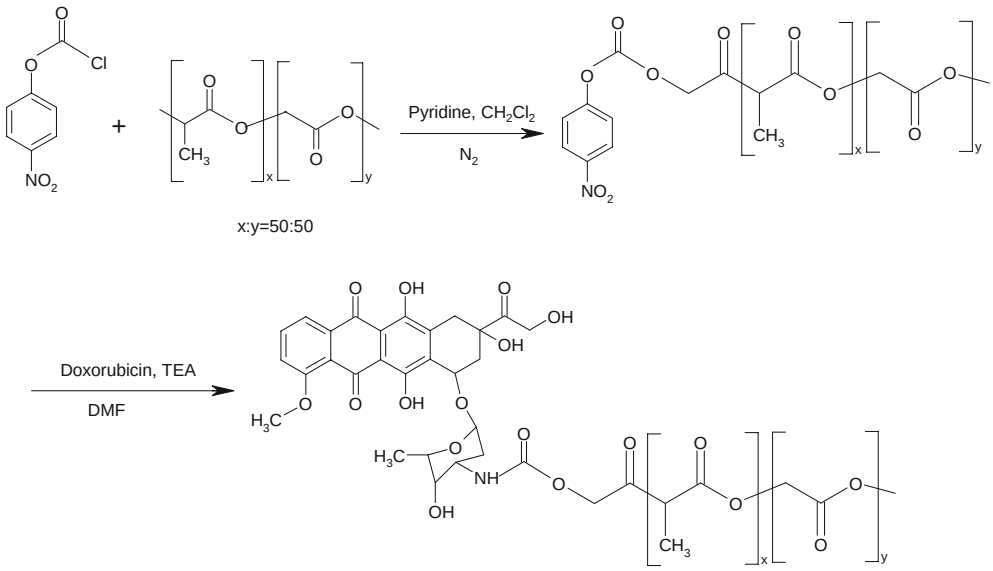

Fig. 1. Scheme of conjugating doxorubicin to PLGA.

Synthesis and Characterization of Doxo-PLGA-PEG-cRGD Nanoparticle

The schematic procedure of synthesis of Doxo-PLGA-PEG-cRGD nanoparticles is presented in Fig. 2. In the preparation of initial PLGA NPs, PEMA was used as surfactant instead of the conventionally used poly(vinyl alcohol) (PVA) to increase the surface carboxyl groups. Saltzman's group had utilized this surfactant to conjugate antibody onto PLGA NPs' surface, and suggested that PEMA did not significantly change the characters of conventional PLGA NPs prepared with PVA (23). The surface modification with PEG and cRGD makes the PLGA nanoparticles more functional than the conventional unmodified PLGA nanoparticles. The characteristics of PLGA nanoparticle (including conjugated doxorubicin) (PLGA-Doxo) and Doxo-PLGA-PEG-cRGD nanoparticle are summarized in Table I. It is obvious that after two steps of conjugation to the PLGA-Doxo NPs surface with PEG and cRGD, the mean size of NPs increased, and also the polydistribution became slightly wider. The surface charge of NPs dramatically increases from −51.7±3.1 to −18.9±2.4 mV, which was attributed to the surface modification with PEG and cRGD, both of them consumed the carboxyl groups on the nanoparticle' surface. However, the surface modification did not significantly change the drug encapsulation efficiency (E.E.) and encapsulation capacity (E.C.), indicating that the formulation and series of modification procedures did not lead to dramatic drug loss, whilst the minor decrease of both E.E. and E.C. may be owing to the loss of unencapsulated doxorubicin conjugates available on particle surface, or the minor amount of doxorubicin cleaved from PLGA during the preparation period, due to the slow hydrolysis of liable glycol block on PLGA backbone in aqueous environment.

The morphology of as-prepared PLGA-Doxo and Doxo-PLGA-PEG-cRGD nanoparticles were characterized by

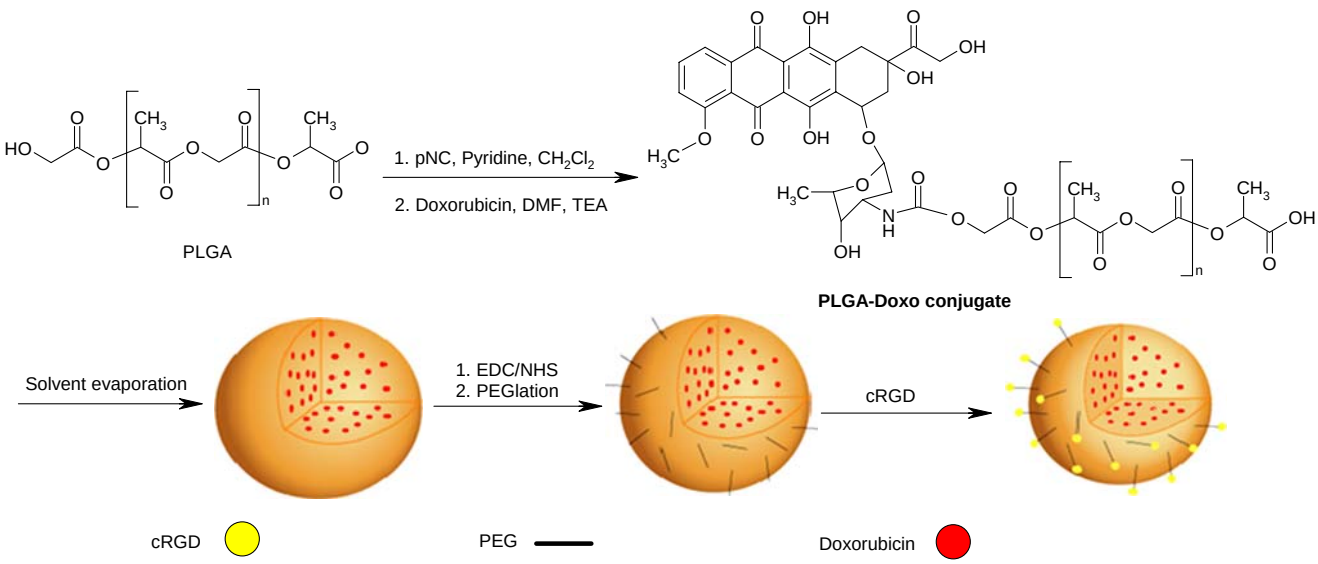

Fig. 2. Schematic route of preparation of Doxo-PLGA-PEG-cRGD nanoparticles.

Table I. Physical Characteristics of PLGA Based Nanoparticles (Mean ± SD, n=3)

	Size (nm)	Poly dispersity	Zeta potential (mV)	E. E.[a] (%)	E. C.[b] (μg drug/mg NP)	cRGD Quantity (nmol peptide/mg NPs)
PLGA-Doxo	366.6±3.1	0.158	−51.7±3.1	88.3	15.32±1.2	N/A
Doxo-PLGA-PEG-cRGD	423.0±16.6	0.189	−18.9±2.4	87.2	14.99±2.4	0.15±0.3

[a] Encapsulation efficiency: drug encapsulated in the NP to initially added drug into the formulation
[b] Encapsulation capacity: the amount of drug encapsulated into milligram of NP

TEM, respectively. It can be seen from Fig. 3 that both types of NP were quite uniform and well-dispersed with low size distribution, similar to the results characterized by dynamic light scattering method (zetasizer measurement). Also, both NPs were solid, spherical nanoparticles with smooth surface.

Cytotoxicity of NPs to Various Malignant Cancer Cells

The cytotoxicity effects of both pure doxorubicin and drug containing nanoparticles were conducted by an established MTT assay (Fig. 4). The drug concentration range was from 0.005 μg/ml to 50 μg/ml. Equivalent amounts of drug encapsulated in drug containing nanoparticles were adjusted to the equivalent concentrations by the corresponding cell culture medium. Cytotoxicity of the drug free NPs was also investigated at the highest NPs concentration used in the MTT assay.

In term of IC_{50} values, the three *integrin* expressing cancer cells retained different sensitivity to pure doxorubicin and Doxo-PLGA-PEG-cRGD NPs, respectively. With pure doxorubicin, B16F10 cells showed the most sensitivity (IC_{50}= 0.09 μg/ml), whilst DU145 (IC_{50}=0.71 μg/ml) and MDA-MB-231 (IC_{50}=0.41 μg/ml) cells presented similar, but lower sensitivity. However, this cytotoxicity trend dramatically changed when cells were treated with Doxo-PLGA-PEG-cRGD nanoparticles. After incubation with NPs, the NPs showed the most cytotoxic to MDA-MB-231 (IC_{50}=0.63 μg/ml), median with B16F10 (IC_{50}=1.13 μg/ml), and the lowest with DU145 (IC_{50}=2.29 μg/ml). It can be seen that for all the three *integrin* expressing cells, the cytotoxic efficacy of the Doxo-PLGA-PEG-cRGD nanoparticles was lower than that of the pure doxorubicin. The cytotoxicity of PLGA-Doxo NPs to these cancer cells was also tested (data not shown), which presented similar but slightly lower efficacy to all the above cancer cells, when compared to the Doxo-PLGA-PEG-cRGD NPs.

Cell Affinity Assay

Affinity of different malignant cells to pure drug, modified and non-modified NPs was investigated by CLSM. Fig. 5a–i shows the uptake of Doxo-PLGA-PEG-cRGD NPs at various time points by different cancer cells. Since B16F10 (24,25), DU145 (26) and MDA-MB-231(27) cells all express αvβ3 *integrin* on cell membranes, Doxo-PLGA-PEG-cRGD NPs should be selectively recognized by these *integrin* expressing cancer cells upon exposure, and underwent endocytotic pathway into cytoplasm. As shown in Fig. 5a–i, the uptake of NPs into cytoplasm followed a time-dependent manner. It was noted that the uptake of NPs was not significant after 2-h incubation, compared to that at 0.5 h. The most significant uptake of NPs was observed at 4 h incubation in B16F10, DU145 and MDA-MB-23 cells. Because of the lacking of *integrin* on MCF-7 cell membrane (28), the uptake of cRGD modified NPs into these cells was few over the 4-h incubation period, except for few non-specific association to cells after 4 h.

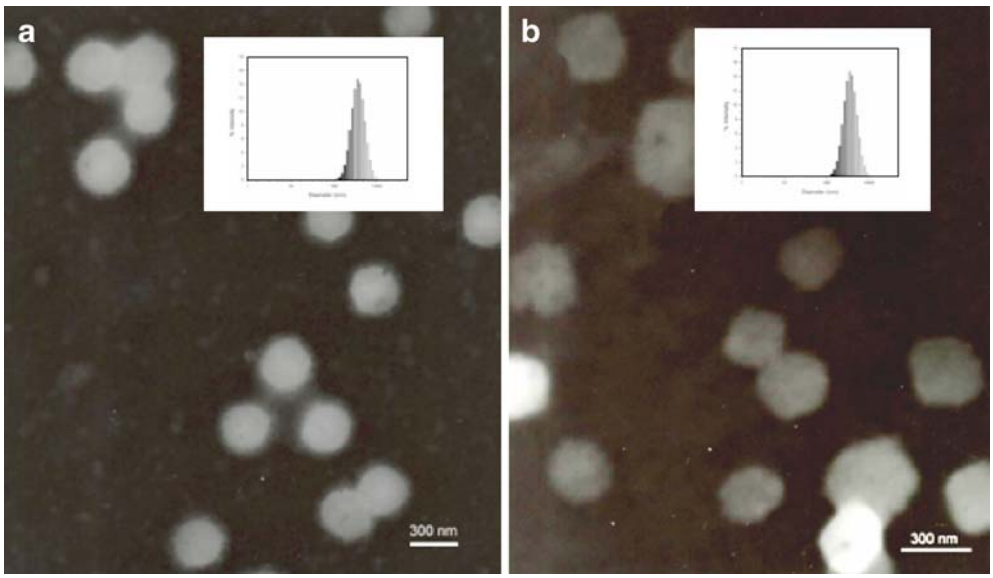

Fig. 3. TEM images of PLGA-Doxo nanoparticles (**a**) and Doxo-PLGA-PEG-cRGD nanoparticles (**b**). *Insets* are the corresponding dynamic light scattering results obtained from measurement of zetasizer.

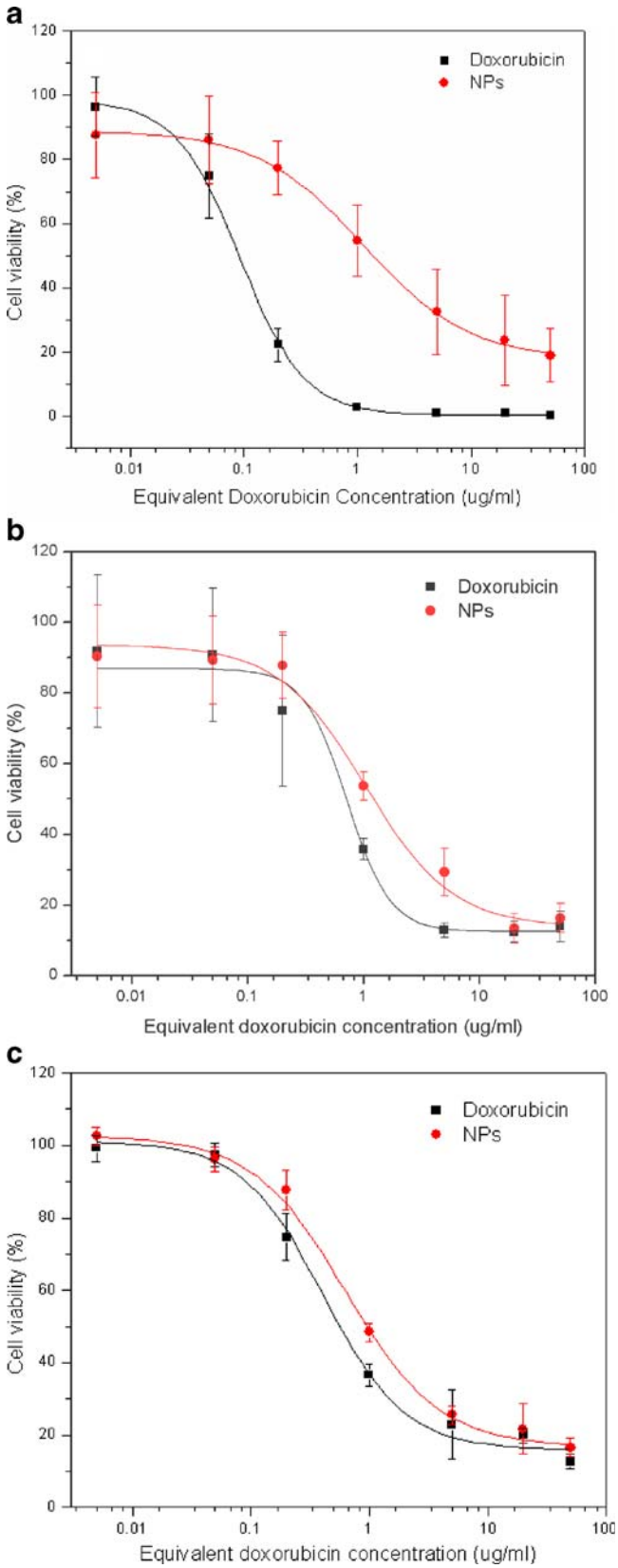

Fig. 4. Cytotoxicity results of Doxo-PLGA-PEG-cRGD nanoparticles or doxorubicin to **a** B16F10 cells, **b** DU145 cells, and **c** MDA-MB-231 cells.

The resultant 1-h uptake effect of Doxo-PLGA-PEG-cRGD NPs, PLGA-PEG NPs, and doxorubicin alone were also compared. It was found that all of the *integrin* expressing cells showed significant uptake of Doxo-PLGA-PEG-cRGD NPs, whilst the uptake of PLGA-PEG NPs and doxorubicin alone remained low (Figures not shown).

In vitro Drug Release

The *in vitro* drug release profile of Doxo-PLGA-PEG-cRGD NPs is shown in Fig. 6. The drug released from the polymer matrix was in a sustained release manner. The "burst release effect" commonly associated with micro- or nanoparticle delivery system was, to some extent, avoided during the first several hours' release period.

Cell Apoptosis Induced by Doxo-PLGA-PEG-cRGD NPs

Typical apoptotic cell death can be detected by various morphological and biochemical characterization of cell death. In this study, agrose gel electrophoresis and western blot were employed to detect Doxo-PLGA-PEG-cRGD NPs induced apoptosis of the cancer cells.

DNA fragmentation effect of Doxo-PLGA-PEG-cRGD NPs was determined on MDA-MB-231 cell line. The respective pure doxorubicin and NPs were adjusted to contain 5 μg/ml of doxorubicin; and the cells were treated with the test solutions for 4 h followed by 44 h incubation in culture media. In Fig. 7, the cells treated with NPs were shown to have more lower-molecular weight (LMW) DNA fragments that were resolved at the bottom of the agrose gel. In contrast, the cells treated with doxorubicin alone had more higher-molecular weight (HMW) DNA fragments found close to the loading well on the gel. Fig. 8 shows the western blot results in which the Doxo-PLGA-PEG-cRGD NPs treated group showed higher cleaved caspase 3 expression.

DISCUSSION

Many patients undertaking chemotherapy are suffering from serious side-effect arising from the anticancer drugs, and some may die because of the side-effect of drugs rather than the cancer itself. Thus, it entails intelligent design of drug delivery system so as to selectively target the conventional chemotherapeutical drugs to the malignant tumor cells with high delivery efficiency and good efficacy so at to overcome the notorious side effects commonly associated with most anticancer drugs. *Integrin*, like $\alpha v\beta 3$, has been extensively investigated to target many malignant cancer cells or endothelial cells for delivering cytotoxic drugs (3–5,29,30). Besides, *integrin* also has profound impacts in angiogenesis and metastasis of many cancers (31). As one of the conventional chemotherapeutical drugs, doxorubicin, an anthracycline antibiotic, is widely used clinically. Despite of its good efficacy for treatment of various cancers, doxorubicin has severe short- and long-term side effects mostly associated with bone marrow and myocardial cytotoxicity (32,33). Thus, doxorubicin conjugates are believed to hold promise to overcome the side effects, and enhance drug efficacy to cancers. It was reported that doxorubicin conjugated novel targeting peptide had significantly improved the therapeutic

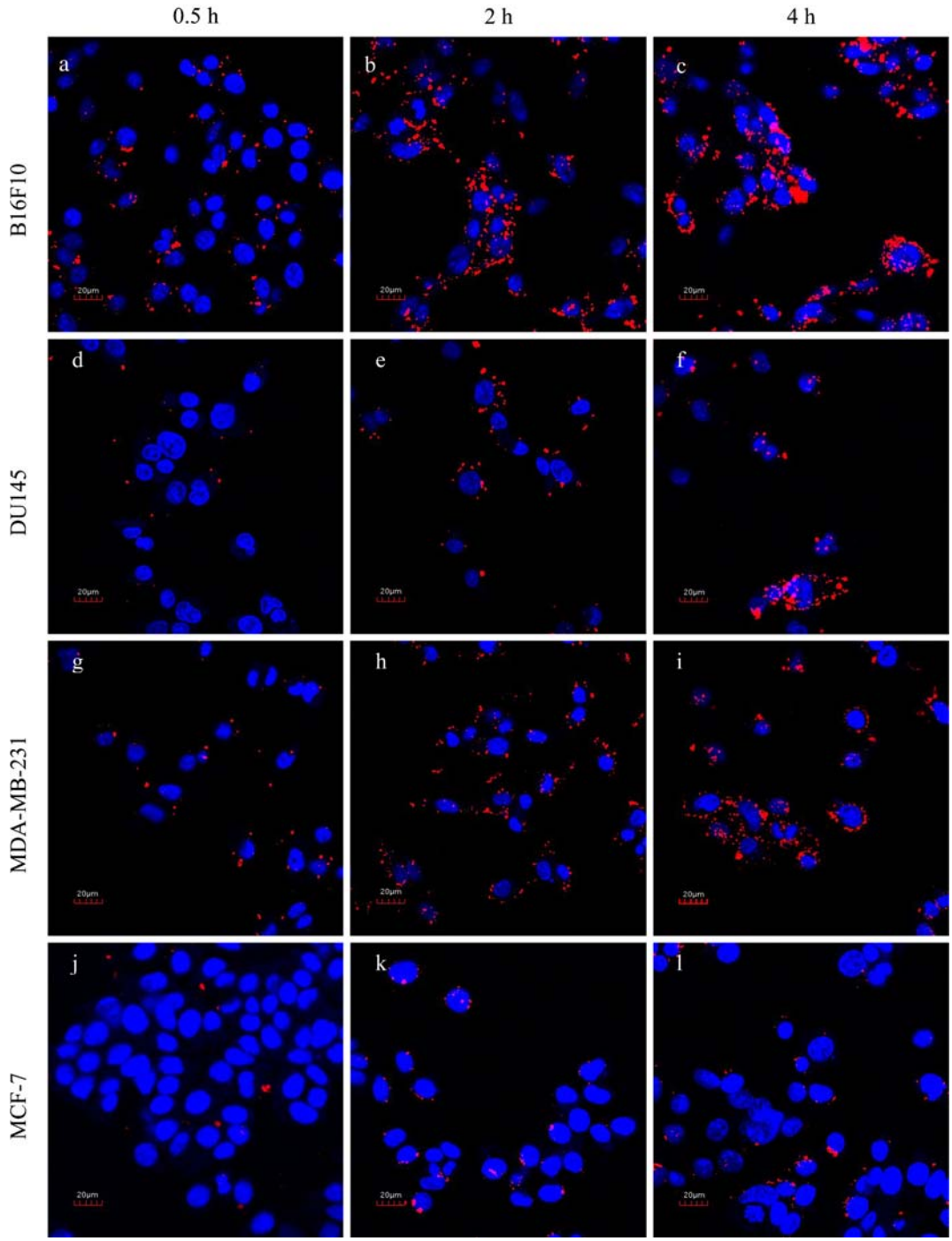

Fig. 5. CLSM results of cellular uptake of Doxo-PLGA-PEG-cRGD nanoparticle in 0.5, 2 and 4 h incubation of **a–c** B16F10 cells, **d–f** DU145 cells, **g–i** MDA-MB-231 cells, and **j–l** MCF-7 cells.

efficacy (33), and water soluble poly(N-(2-hydroxy-propyl) methacrylamide) (HPMA) polymer based conjugates has also been extensively studied (34–37), and some are under phase I clinical evaluation (34,38). RGD peptide, one of the small bioactive molecules, is typically favored by many researchers as targeting ligand to deliver pay-loads to targeted sites (20,39).

Nowadays, various PLGA based drug/gene delivery systems with a variety of ligands have been investigated, whereas few reports have focused on fabrication of PLGA NPs with both active and passive targeting moieties simultaneously for treating malignant cancers. In this study, we fabricated the PLGA based doxorubicin delivery system with both passive and active targeting functions for malignant *integrin* expressing cancer cells. PEG (2000 M.W.) was chosen to realize the passive purpose, as PEG was reported to have the least protein interaction in animal body, was able to prolong the circulation period of pharmaceuticals, and was still functional at the distal end (40–43). The molecular weight of 2000 Dalton was chosen, as PEG of higher molecular weight might hinder the cRGD active targeting function (28). The dynamic light scattering and TEM analysis showed that

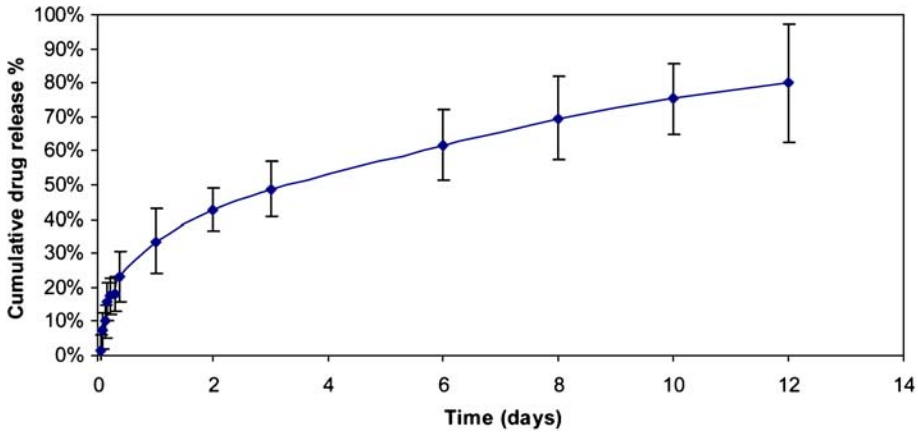

Fig. 6. *In vitro* drug release profile of Doxo-PLGA-PEG-cRGD nanoparticles over 12 days at 37°C, 100 rpm in shaking water bath. Results are represented in triplicate.

the as-synthesized Doxo-PLGA-PEG-cRGD NPs were uniform and well-dispersed; both properties are prerequisites for drug delivery systems suitable for clinical applications. Doxorubicin has moderate water solubility, whereas PLGA is rather hydrophobic. Thus, it is difficult to incorporate doxorubicin into PLGA NPs in high efficiency. Conjugation doxorubicin to one of the distal ends of PLGA significantly enhanced the loading efficiency from less than 1% (44) to 87.2% as found in this study.

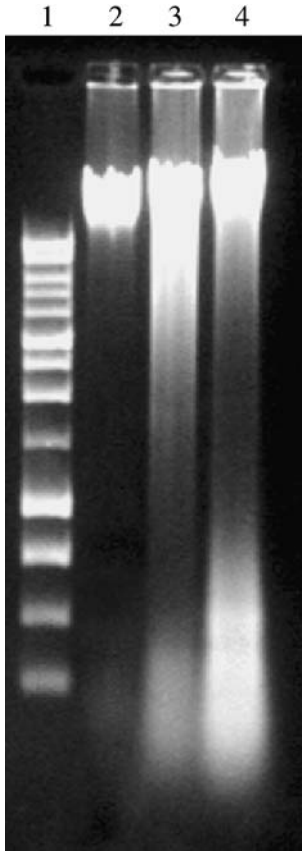

Fig. 7. DNA fragment results from agarose gel electrophoresis. Lane *1* DNA ladder, Lane *2* MDA-MB-231 cells treated with cell culture medium, Lane *3* MDA-MB-231 cells treated with doxorubicin, Lane *4* MDA-MB-231 cells treated with Doxo-PLGA-PEG-cRGD nanoparticles.

The different cytotoxic effects of Doxo-PLGA-PEG-cRGD NPs to various malignant *integrin* expressing cancer cells were probably caused by the different *integrin* receptor expression levels on the cell membranes, with MDA-MB-231 the highest and DU145 the lowest (34–37), leading to different uptake efficiency of NPs. Also, the particulated doxorubicin delivery system altered the uptake of doxorubicin into cytoplasma from diffusion for pure doxorubicin aqueous solution to endocytosis pathway for doxorubicin containing NPs. What's more, with the cRGD modification on NPs surface, the threshold for cytotoxic onset may be changed, as the cRGD is also an *integrin* inhibitor at appropriate concentrations in tumor microenvironment (45). The inherent different cellular sensitivity to pure drug could also influence the resultant IC_{50} values of the drug loaded NPs. When a cell is already very sensitive to a drug, the advantage of formulating the drug into NP delivery system may not be very evident *in vitro*. As reported by other researchers (19), the conjugation of doxorubicin to PLGA polyester led to compromised cytotoxic effect to cancer cells (Fig. 4). In this study, Doxo-PLGA-PEG-cRGD showed the least compromised efficacy to MDA-MB-231 cells, which may result from the higher *integrin* expression level in that cell line facilitating the uptake of NPs into cytoplasma, and/or the less sensitivity of this cell line to pure doxorubicin. When a cell is less sensitive to a drug, the advantage of adding a targeting moiety to the delivery system will become more evident *in vitro*, and recovers some of the compromised effects due to the NP fabrication.

Results from CLSM (Fig. 5) revealed that Doxo-PLGA-PEG-cRGD NPs were preferred to be up-taken by MDA-MB-231 and B16F10 cells that had overexpressed *integrin* on their cell membranes. However, the uptake efficiency became static for both cells at a longer incubation time (no apparent

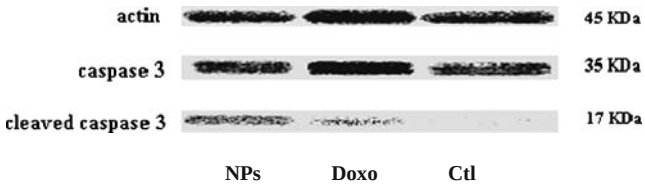

Fig. 8. Western Blot results: *NPs* Doxo-PLGA-PEG-cRGD nanoparticles, *Doxo* doxorubicin, *Ctl* culture medium.

difference in uptake after 4-h incubation with NPs); this might be due to saturation of the cellular surface receptor for NPs (30). Results from flow cytometry also showed the increasing uptake of Doxo-PLGA-PEG-cRGD NPs with ascending concentration of NPs (data not shown).

The DNA fragmentation phenomenon is involved in most apoptotic conditions. Cells undergoing apoptosis process often produce short DNA fragments as indicated in our result (Fig. 7). Doxo-PLGA-PEG-cRGD NPs showed the most potency to induce dramatic DNA fragmentation compared with doxorubicin alone. Cysteine proteases of the caspase family also play vital roles in the execution of apoptosis. Amongst the caspase family, caspase 3 acts as executor in apoptosis, leading to series of subsequent apoptotic signaling pathways (46). Fig. 8 shows that higher activated caspase 3 expression level was found in the cells treated with the Doxo-PLGA-PEG-cRGD NPs. Therefore, the results from DNA fragmentation assay and western blot confirmed that Doxo-PLGA-PEG-cRGD NPs were able to deliver chemotherapeutical drugs selectively to the *integrin* expressing cancer cells and induce apoptosis in these cells.

Although the cytotoxic efficacy of doxorubicin was compromised after conjugation to PLGA, the selective targeting property and the sustained drug release profile of the doxorubicin NPs could improve the efficacy of the drug *in vivo*. The release kinetics of doxorubicin from the formulation was in zero-order (R^2=0.97), in the range from 12 h to 12 days (Fig. 6). The release mechanism was assumed to be due to a combination of chemical degradation and diffusion release (19).

CONCLUSION

In this study, two independent approaches that conjugating doxorubicin to PLGA and mounting active and passive targeting moieties with PEG and cRGD onto to the NPs were adopted to fabricate the Doxo-PLGA-PEG-cRGD NPs. The NPs synthesized in this study were proven able to effectively target doxorubicin to malignanat *integrin* expressing cancer cells, and showed profound apoptotic induction effect to those cells. Although the drug efficacy to cancer cells was compromised after conjugation with PLGA, the resultant sustained release behavior and the property of selective uptake of the NPs by cancer cells could still make Doxo-PLGA-PEG-cRGD NPs a good candidate for anticancer therapy.

ACKNOWLEDGMENT

This study was supported by Academic Research Funding, grant number R148-000-097-112. Z. Wang is grateful to National University of Singapore for the financial support to his graduate studies.

REFERENCES

1. R. O. Hynes. Integrins: bidirectional, allosteric signaling machines. *Cell*. **110**:673–687 (2002). doi:10.1016/S0092-8674(02)00971-6.
2. R. O. Hynes. Integrins: versatility, modulation, and signaling in cell adhesion. *Cell*. **69**:11–25 (1992). doi:10.1016/0092-8674(92)90115-S.
3. R. M. Schiffelers, G. A. Koning, T. L. M. ten Hagen, M. Fens, A. J. Schraa, A. Janssen, R. J. Kok, G. Molema, and G. Storm. Anti-tumor efficacy of tumor vasculature-targeted liposomal doxorubicin. *J Control Release*. **91**:115–122 (2003). doi:10.1016/S0168-3659(03)00240-2.
4. R. M. Schiffelers, A. Ansari, J. Xu, Q. Zhou, Q. Q. Tang, G. Storm, G. Molema, P. Y. Lu, P. V. Scaria, and M. C. Woodle. Cancer siRNA therapy by tumor selective delivery with ligand-targeted sterically stabilized nanoparticle. *Nucleic Acids Res*. **32**:e149 (2004). doi:10.1093/nar/gnh140.
5. K. Temming, R. M. Schiffelers, G. Molema, and R. J. Kok. RGD-based strategies for selective delivery of therapeutics and imaging agents to the tumour vasculature. *Drug Resist Updat*. **8**:381–402 (2005). doi:10.1016/j.drup.2005.10.002.
6. K. Temming, D. L. Meyer, R. Zabinski, E. C. Dijkers, K. Poelstra, G. Molema, and R. J. Kok. Evaluation of RGD-targeted albumin carriers for specific delivery of auristatin E to tumor blood vessels. *Bioconjug Chem*. **17**:1385–1394 (2006). doi:10.1021/bc060087z.
7. P. M. Winter, S. D. Caruthers, A. Kassner, T. D. Harris, L. K. Chinen, J. S. Allen, E. K. Lacy, H. Zhang, J. D. Robertson, S. A. Wickline, and G. M. Lanza. Molecular imaging of angiogenesis in nascent Vx-2 rabbit tumors using a novel alpha(nu)beta3-targeted nanoparticle and 1.5 tesla magnetic resonance imaging. *Cancer Res*. **63**:5838–5843 (2003).
8. R. Langer. Drug delivery. Drugs on target. *Science*. **293**:58–59 (2001). doi:10.1126/science.1063273.
9. M. E. Davis, Z. Chen, and D. M. Shin. Nanoparticle therapeutics: an emerging treatment modality for cancer. *Nature Reviews Drug Discovery*. **7**:771–782 (2008). doi:10.1038/nrd2614.
10. T. Lammers, W. E. Hennink, and G. Storm. Tumour-targeted nanomedicines: principles and practice. *Br. J. Cancer*. **99**:392–397 (2008). doi:10.1038/sj.bjc.6604483.
11. K. J. Cho, X. Wang, S. M. Nie, Z. Chen, and D. M. Shin. Therapeutic nanoparticles for drug delivery in cancer. *Clin Cancer Res*. **14**:1310–1316 (2008). doi:10.1158/1078-0432.CCR-07-1441.
12. S. Dandamudiand, and R. B. Campbell. The drug loading, cytotoxicty and tumor vascular targeting characteristics of magnetite in magnetic drug targeting. *Biomaterials*. **28**:4673–83 (2007). doi:10.1016/j.biomaterials.2007.07.024.
13. G. S. Papaetis, C. Roussos, and K. N. Syrigos. Targeted therapies for non-small cell lung cancer. *Curr. Pharm. Des*. **13**:2810–2831 (2007). doi:10.2174/138161207781757079.
14. S. H. Kim, J. H. Jeong, K. W. Chun, and T. G. Park. Target-specific cellular uptake of PLGA nanoparticles coated with poly (L-lysine)-poly(ethylene glycol)-folate conjugate. *Langmuir*. **21**:8852–8857 (2005). doi:10.1021/la0502084.
15. Y. Bae, N. Nishiyama, and K. Kataoka. *In vivo* antitumor activity of the folate-conjugated pH-sensitive polymeric micelle selectively releasing adriamycin in the intracellular acidic compartments. *Bioconjug. Chem*. **18**:1131–1139 (2007). doi:10.1021/bc060401p.
16. D. Peer, J. M. Karp, S. Hong, O. C. FaroKhzad, R. Margalit, and R. Langer. Nanocarriers as an emerging platform for cancer therapy. *Nature Nanotech*. **2**:751–760 (2007). doi:10.1038/nnano.2007.387.
17. H. S. Yoo, K. H. Lee, J. E. Oh, and T. G. Park. *In vitro* and *in vivo* anti-tumor activities of nanoparticles based on doxorubicin-PLGA conjugates. *J. Control. Release*. **68**:419–31 (2000). doi:10.1016/S0168-3659(00)00280-7.
18. J. E. Oh, Y. S. Nam, K. H. Lee, and T. G. Park. Conjugation of drug to poly(D,L-lactic-co-glycolic acid) for controlled release from biodegradable microspheres. *J. Control. Release*. **57**:269–280 (1999). doi:10.1016/S0168-3659(98)00123-0.
19. H. S. Yoo, J. E. Oh, K. H. Lee, and T. G. Park. Biodegradable nanoparticles containing doxorubicin-PLGA conjugate for sustained release. *Pharm. Res*. **16**:1114–8 (1999). doi:10.1023/A:1018908421434.
20. N. Zhang, C. Chittasupho, C. Duangrat, T. J. Siahaan, and C. Berkland. PLGA nanoparticle–peptide conjugate effectively targets intercellular cell-adhesion molecule-1. *Bioconjug. Chem*. **19**:145–152 (2008). doi:10.1021/bc700227z.
21. F. Chen, Y. Liu, J. Lu, K. J. Hwang, and V. H. Lee. A sensitive fluorometric assay for reducing sugars. *Life Sci*. **50**:651–659 (1992). doi:10.1016/0024-3205(92)90450-4.

22. M. Herrmann, H. M. Lorenz, R. Voll, M. Grunke, W. Woith, and J. R. Kalden. A rapid and simple method for the isolation of apoptotic DNA fragments. *Nucleic Acids Res*. **22**:5506–5507 (1994). doi:10.1093/nar/22.24.5506.
23. M. E. Keegan, S. M. Royce, T. Fahmy, and W. M. Saltzman. *In vitro* evaluation of biodegradable microspheres with surface-bound ligands. *J. Control. Release*. **110**:574–580 (2006). doi:10.1016/j.jconrel.2005.11.004.
24. L. Vellon, J. A. Menendez, H. Liu, and R. Lupu. Up-regulation of alphavbeta3 integrin expression is a novel molecular response to chemotherapy-induced cell damage in a heregulin-dependent manner. *Differentiation*. **75**:819–830 (2007). doi:10.1111/j.1432-0436.2007.00241.x.
25. O. H. Ramos, A. Kauskot, M. R. Cominetti, I. Bechyne, C. L. Salla Pontes, F. Chareyre, J. Manent, R. Vassy, M. Giovannini, C. Legrand, H. S. Selistre-de-Araujo, M. Crepin, and A. Bonnefoy. A novel alpha(v)beta (3)-blocking disintegrin containing the RGD motive, DisBa-01, inhibits bFGF-induced angiogenesis and melanoma metastasis. *Clin. Exp. Metastasis*. **25**:53–64 (2008). doi:10.1007/s10585-007-9101-y.
26. B. R. Line, A. Mitra, A. Nan, and H. Ghandehari. Targeting tumor angiogenesis: Ccomparison of peptide and polymer-peptide conjugates. *J. Nucl. Med*. **46**:1552–1560 (2005).
27. R. S. Yang, C. H. Tang, W. J. Chuang, T. H. Huang, H. C. Peng, T. F. Huang, and W. M. Fu. Inhibition of tumor formation by snake venom disintegrin. *Toxicon*. **45**:661–669 (2005). doi:10.1016/j.toxicon.2005.01.013.
28. W. Cai, D. W. Shin, K. Chen, O. Gheysens, Q. Cao, S. X. Wang, S. S. Gambhir, and X. Chen. Peptide-labeled near-infrared quantum dots for imaging tumor vasculature in living subjects. *Nano Lett*. **6**:669–676 (2006). doi:10.1021/nl052405t.
29. C. B. Pattillo, F. Sari-Sarraf, R. Nallamothu, B. M. Moore, G. C. Wood, and M. F. Kiani. Targeting of the antivascular drug combretastatin to irradiated tumors results in tumor growth delay. *Pharm. Res*. **22**:1117–1120 (2005). doi:10.1007/s11095-005-5646-0.
30. W. Arap, R. Pasqualini, and E. Ruoslahti. Cancer treatment by targeted drug delivery to tumor vasculature in a mouse model. *Science*. **279**:377–380 (1998). doi:10.1126/science.279. 5349.377.
31. E. A. Murphy, B. K. Majeti, L. A. Barnes, M. Makale, S. M. Weis, K. Lutu-Fuga, W. Wrasidlo, and D. A. Cheresh. Nanoparticle-mediated drug delivery to tumor vasculature suppresses metastasis. *Proc. Natl. Acad. Sci. U. S. A*. **105**:9343–9348 (2008). doi:10.1073/pnas.0803728105.
32. G. Minotti, P. Menna, E. Salvatorelli, G. Cairo, and L. Gianni. Anthracyclines: molecular advances and pharmacologic developments in antitumor activity and cardiotoxicity. *Pharmacol. Rev*. **56**:185–229 (2004). doi:10.1124/pr.56.2.6.
33. F. Meyer-Losic, J. Quinonero, V. Dubois, B. Alluis, M. Dechambre, M. Michel, F. Cailler, A. M. Fernandez, A. Trouet, and J. Kearsey. Improved therapeutic efficacy of doxorubicin through conjugation with a novel peptide drug delivery technology (Vectocell). *J. Med. Chem*. **49**:6908–6916 (2006). doi:10.1021/jm0606591.
34. B. Rihovaand, and K. Kubackova. Clinical implications of N-(2-hydroxypropyl)methacrylamide copolymers. *Current Pharmaceutical Biotechnology*. **4**:311–322 (2003). doi:10.2174/1389201033489711.
35. T. Lammers, V. Subr, P. Peschke, P. Kuhnlein, W. E. Hennink, K. Ulbrich, F. Kiessling, M. Heilmann, J. Debus, P. E. Huber, and G. Storm. Image-guided and passively tumour-targeted polymeric nanomedicines for radiochemotherapy. *Br. J. Cancer*. **99**:900–910 (2008). doi:10.1038/sj.bjc.6604561.
36. T. Lammers, P. Peschke, R. Kuehnlein, V. Subr, K. Ulbrich, P. Huber, W. Hennink, and G. Storm. Effect of intratumoral injection on the biodistribution and the therapeutic potential of HPMA copolymer-based drug delivery systems. *Neoplasia*. **8**:788–795 (2006). doi:10.1593/neo.06436.
37. R. Duncan. Polymer conjugates as anticancer nanomedicines. *Nat. Rev., Cancer*. **6**:688–701 (2006). doi:10.1038/nrc1958.
38. P. A. Vasey, S. B. Kaye, R. Morrison, C. Twelves, P. Wilson, R. Duncan, A. H. Thomson, L. S. Murray, T. E. Hilditch, T. Murray, S. Burtles, D. Fraier, E. Frigerio, and J. Cassidy. Phase I clinical and pharmacokinetic study of PK1 [N-(2-hydroxypropyl)-methacrylamide copolymer doxorubicin]: first member of a new class of chemotherapeutic agents-drug-polymer conjugates. Cancer Research Campaign Phase I/II Committee. *Clin. Cancer Res*. **5**:83–94 (1999).
39. C. Deng, H. Y. Tian, P. B. Zhang, J. Sun, X. S. Chen, and X. B. Jing. Synthesis and characterization of RGD peptide grafted poly (ethylene glycol)-b-poly(L-lactide)-b-poly(L-glutamic acid) triblock copolymer. *Biomacromolecules*. **7**:590–596 (2006). doi:10.1021/bm050678c.
40. O. C. Farokhzad, J. J. Cheng, B. A. Teply, I. Sherifi, S. Jon, P. W. Kantoff, J. P. Richie, and R. Langer. Targeted nanoparticle-aptamer bioconjugates for cancer chemotherapy *in vivo*. *Proc. Natl. Acad. Sci. U. S. A*. **103**:6315–6320 (2006). doi:10.1073/pnas.0601755103.
41. K. Avgoustakis. Pegylated poly(lactide) and poly(lactide-co-glycolide) nanoparticles: Preparation, properties and possible applications in drug delivery. *Current Drug Delivery*. **1**:321–333 (2004). doi:10.2174/1567201043334605.
42. L. E. van Vlerken, T. K. Vyas, and M. M. Amiji. Poly(ethylene glycol)-modified nanocarriers for tumor-targeted and intracellular delivery. *Pharm. Res*. **24**:1405–1414 (2007). doi:10.1007/s11095-007-9284-6.
43. S. M. Ryan, G. Mantovani, X. X. Wang, D. M. Haddleton, and D. J. Brayden. Advances in PEGylation of important biotech molecules: delivery aspects. *Expert Opinion on Drug Delivery*. **5**:371–383 (2008). doi:10.1517/17425247.5.4.371.
44. S. Sengupta, D. Eavarone, I. Capila, G. Zhao, N. Watson, T. Kiziltepe, and R. Sasisekharan. Temporal targeting of tumour cells and neovasculature with a nanoscale delivery system. *Nature*. **436**:568–572 (2005). doi:10.1038/nature03794.
45. S. Strieth, M. E. Eichhorn, A. Sutter, A. Jonczyk, A. Berghaus, and M. Dellian. Antiangiogenic combination tumor therapy blocking alpha(v)-integrins and VEGF-receptor-2 increases therapeutic effects *in vivo*. *Int. J. Cancer*. **119**:423–431 (2006). doi:10.1002/ijc.21838.
46. M. Kim, J. Liao, M. L. Dowling, K. R. Voong, S. E. Parker, S. Wang, W. S. El-Deiry, and G. D. Kao. TRAIL inactivates the mitotic checkpoint and potentiates death induced by microtubule-targeting agents in human cancer cells. *Cancer Res*. **68**:3440–3449 (2008). doi:10.1158/0008-5472.CAN-08-0014.